

## Supporting Information

### **Acetaldehyde as an Intermediate in the Electroreduction of Carbon Monoxide to Ethanol on Oxide-Derived Copper**

*Erlend Bertheussen, Arnau Verdaguer-Casadevall, Davide Ravasio, Joseph H. Montoya, Daniel B. Trimarco, Claudie Roy, Sebastian Meier, Jürgen Wendland, Jens K. Nørskov, Ifan E. L. Stephens,\* and Ib Chorkendorff\**

anie\_201508851\_sm\_miscellaneous\_information.pdf

## **S.1 Electrode Preparation**

5x10 mm electrodes were cut from a 100x100 mm foil (Alfa Aesar Supratronic®, ≥ 99.9999 %, 0.1 mm thickness) and attached to a Cu wire (Goodfellow, ≥ 99.999 %, 0.5 mm diameter). An electropolishing procedure was then carried out at 2.1 V vs. a Pt counter electrode placed ~2 cm from the working electrode in a 1:2 solution of phosphoric acid (Merck EMSURE®, 85 %) in water (Millipore Synergy®) for two minutes. Then they were annealed in air at 500 °C for an hour and slowly cooled. Finally, they were reduced chronopotentiometrically at  $-7 \text{ mA cm}^{-2}$  in 0.1 M KOH (Fluka TraceSELECT®, ≥ 99.995 %) electrolyte.

## S.2 Capacitance Surface Area Measurements

The electrochemically active surface area of the OD-Cu electrodes was estimated from the capacitance current in the non-faradaic regime of cyclic voltammograms measured at different scan rates. By plotting capacitance current against scan rate, the capacitance of the surface can be obtained through the slope of the linear fit.<sup>[1]</sup> In figure S.1, the CVs obtained in a representative measurement on OD-Cu are shown. The average capacitance of the OD-Cu electrodes was  $23.1 \pm 2.7 \text{ mF cm}^{-2}$ . Similar measurements were carried out for polycrystalline Cu electrodes, as illustrated in figure S.7, yielding  $264 \mu\text{F cm}^{-2}$  as a reference value.

By assuming that electropolished polycrystalline copper foils are atomically flat, the surface area of the OD-Cu electrodes can be determined by comparing the two different capacitance values. This was done for 7 different electrodes, yielding an average roughness factor of  $87 \pm 10$ . This value was used to normalize the current density to the electrochemical surface area, shown in figure 1 (b) in the main article. Note that these measurements are carried out before CO reduction measurements. The capacitance of the OD-Cu electrodes change during electrolysis.<sup>[1]</sup>

It is worth noting that both the oxide-derived and polycrystalline Cu values are significantly higher than what was reported by Li et al.<sup>[1]</sup> However, previous work by Koper and coworkers on copper single crystals show similar capacitance values to those obtained for polycrystalline copper in the current work.<sup>[2]</sup> These deviations could mean that the OD-Cu electrodes produced throughout this study were rougher than those previously reported, possibly explaining the higher activity observed.

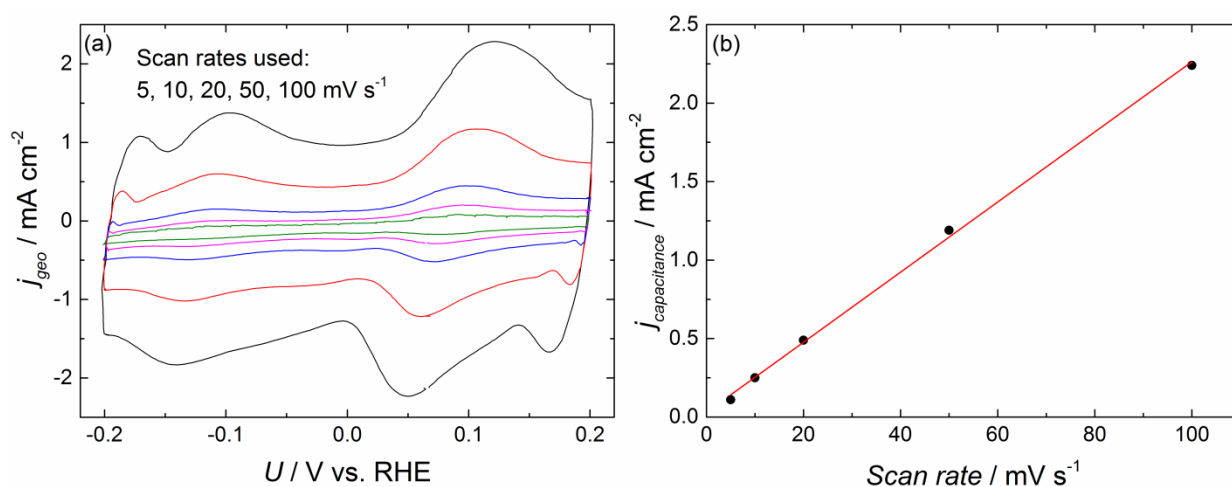


**Figure S.1.** Capacitance measurements on OD-Cu. (a) CVs from a representative OD-Cu sample before CO reduction measurements. Scan rates of 5, 10, 20, 50 and  $100 \text{ mV s}^{-1}$  were used. (b) Capacitance current plotted versus scan rate. The current is obtained at the minimum at  $\sim 0.0 \text{ V}$ . The slope of the linear fit yields the capacitance of the surface, which is  $22.7 \text{ mF cm}^{-2}$  for this electrode.

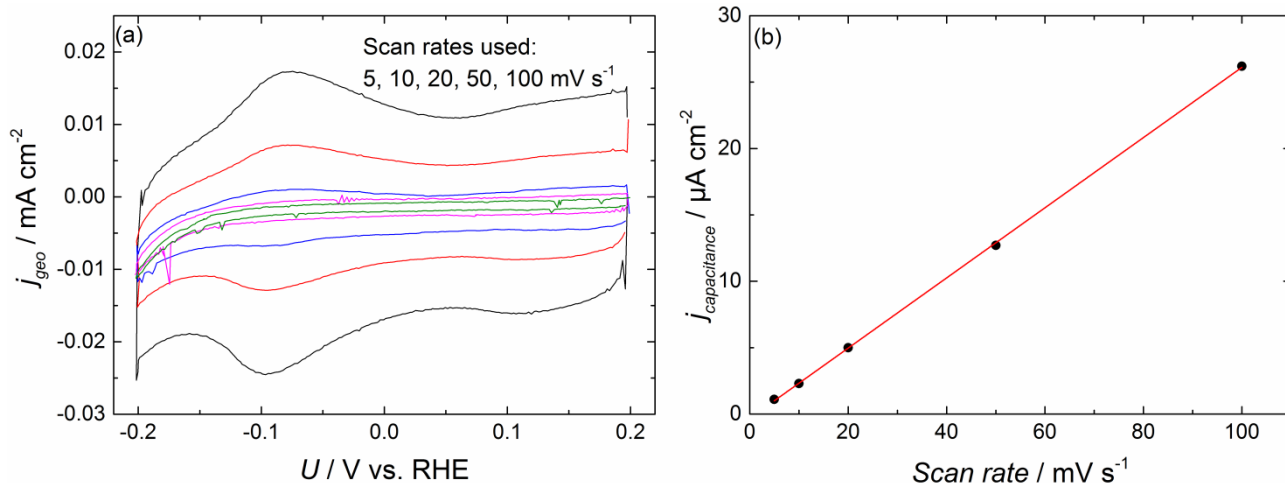


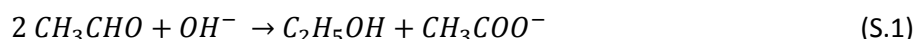
**Figure S.2.** Capacitance measurements on polycrystalline Cu. (a) CVs from a representative polycrystalline Cu. Scan rates of 5, 10, 20, 50 and 100  $\text{mV s}^{-1}$  were used. (b) Capacitance current plotted versus scan rate. The current is obtained at the minimum at  $\sim 0.05$  V. The slope of the linear fit yields the capacitance of the surface, which is 264  $\mu\text{F cm}^{-2}$  in this case.

### S.3 Acetaldehyde Chemistry

The chemistry of aldehydes in alkaline solution is complex.<sup>[3]</sup> When discovering that acetaldehyde was present as a liquid reaction product, but was not detectable in NMR spectra, we tested a number of different hypotheses to explain this.

#### The Cannizzaro Reaction

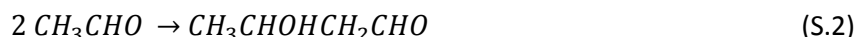
The Cannizzaro reaction is base-catalyzed disproportionation of an aldehyde into the corresponding alcohol and carboxylate ion.<sup>[4]</sup> The reaction scheme for acetaldehyde is shown in equation (S.1).



Ethanol and acetate are two major products from CO electroreduction on OD-Cu. HS-GC-FID is carried out immediately after electrolysis measurements, while NMR spectroscopy is performed some hours later. Since acetaldehyde was detected when using HS-GC, but not in NMR spectroscopy, we hypothesized that it was converted to ethanol and acetate in the time that passed before the latter could be carried out. However, when a standard solution of 10 mM CH<sub>3</sub>CHO in 0.1 M KOH was stored overnight, no ethanol could be detected, as shown in figure S.1.

#### The Aldol Reaction

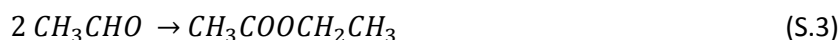
The aldol reaction is a base-catalyzed reaction where two aldehydes condensate to form an aldol.<sup>[5]</sup> In equation (S.2), the reaction scheme with acetaldehyde is shown.



The reaction product is the 3-hydroxybutanal, which is soluble in water. Hence, if the reaction was occurring to a significant extent, this product should appear in NMR spectroscopy. As shown in figure S.10, this is not the case. However, it is likely that aldol condensation occurs to a low degree, contributing to reduction of the acetaldehyde signal, as discussed further below.

#### The Tischenko Reaction

The Tischenko reaction is another disproportionation reaction involving aldehydes, catalyzed by alkoxides. In the case of acetaldehyde, two molecules disproportionate to form a single ethyl acetate molecule, as shown in equation equation (S.3).



As is the case for aldol condensation, this product should be clearly visible in NMR spectra if occurring to a significant extent, which is not the case here.

#### Evaporation

Acetaldehyde is highly volatile. With a boiling point of 20.9 °C,<sup>[6]</sup> its equilibrium phase at room temperature is gaseous. Thus, we hypothesized that it could be evaporating into the relatively large headspace volume of the NMR tubes. However, when diluting a measurement sample from 0.5 to 5 mL after NMR spectroscopy was carried out, and measuring it with HS-GC-FID, acetaldehyde can still be identified, suggesting that evaporation is not significant. A chromatogram from such a measurement on a 250 μM acetaldehyde sample diluted to 25 μM after NMR spectroscopy is shown in figure S.4.

## Polymerization/aggregation

Various other reasons can make the NMR detection of acetaldehyde intermediates in the electroreduction of carbon monoxide to ethanol challenging. As a transient steady state intermediate (see main text figure 3), acetaldehyde never accumulates to appreciable amounts, as opposed to the putative products acetate and ethanol. In addition, acetaldehyde exists in different forms in solution, both as hydrate and free acetaldehyde, thus reducing the sensitivity in the detection of either form due to the NMR resolution of both forms into different signal sets. Basic acetaldehyde solutions undergo aldol reactions to form multifunctional 3-hydroxybutanal and crotonaldehyde with possible ensuing polymerization.<sup>[7]</sup>

For alkaline solutions of acetaldehyde in concentrations higher than ~1 mM, a yellowish color can be observed after some hours. For concentrated solutions ( $\geq 0.1$  M), a dark yellow precipitate forms, as shown in figure S.3 (b). Upon acidification of 500  $\mu$ M acetaldehyde standard solutions prepared from either the 100 % or 40 % precursor (see section S.3 for description of the different acetaldehyde solutions), two broadened signals appear in NMR. When in KOH, NMR spectra from the 100 % solution do not show any acetaldehyde signal above the detection limit, while the standard from the 40 % solution acetaldehyde appears as a sharp doublet at ~1.25 ppm chemical shift, as shown in figure 2 in the main article. A spectrum from an acidified sample of each type is shown in figure S.3 (a). The chemical shifts of the two broad peaks match those of ethyl acetate, which is an acetaldehyde dimer. We interpret the appearance of this compound as an indication of depolymerization occurring in the acidified solution. Based on these different observations, we hypothesize that acetaldehyde polymerizes into larger molecules that can precipitate and/or lead to significant line broadening.

These factors could rationalize the difficulty to detect acetaldehyde as an intermediate in solution. Using extensive spectral accumulation (4096 transients on a 600 MHz Bruker Avance III spectrometer equipped with a BBO smart probe) and the use of an aged acetaldehyde solution (in 0.1 M KOH), we identify several spectral features of the electroreduction sample in the fresh and aged reference spectra (figure S.5), including residual acetaldehyde signals.

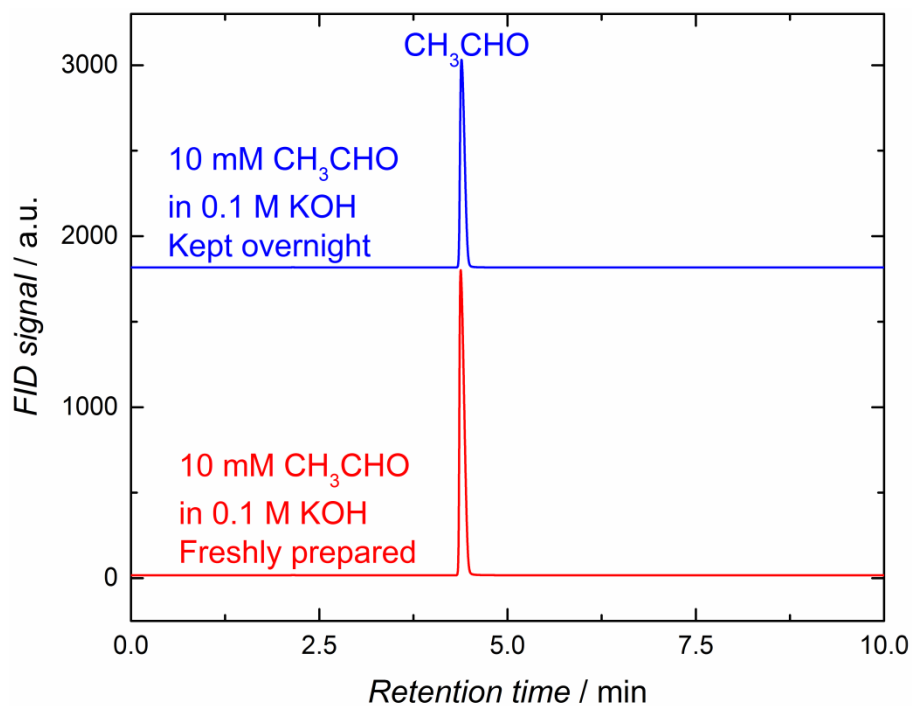


**Figure S.3.** HS-GC-FID measurements to check for Cannizzaro reaction. A standard solution of 10 mM CH<sub>3</sub>CHO was measured right after preparation (red) and after being stored in a closed container overnight (blue). A slight decrease in acetaldehyde concentration can be observed, most likely due to evaporation. However, no ethanol peak appears around 7.8 min retention time, showing that the Cannizzaro reaction is insignificant.

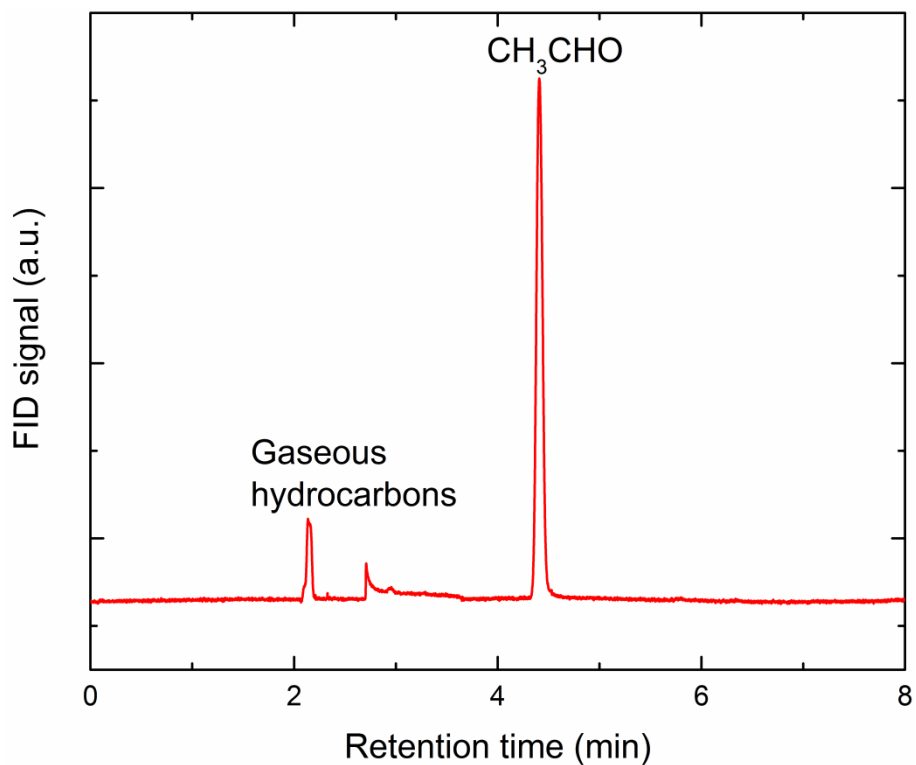


**Figure S.4.** HS-GC-FID measurements to check for evaporation. A 250  $\mu\text{M}$   $\text{CH}_3\text{CHO}$  in 0.1 M KOH sample made from the 100 % precursor (see section S.3 for further discussion about the two different acetaldehyde precursors) was measured using NMR spectroscopy and kept overnight. It was then diluted by a factor of 10 and measured using HS-GC-FID, showing the presence of acetaldehyde, even though it was not visible in NMR spectra (see figure S.3, S.? and figure 2 in the main text). The small peaks between 2 and 3 minutes are caused by gaseous hydrocarbons dissolved in the solution.



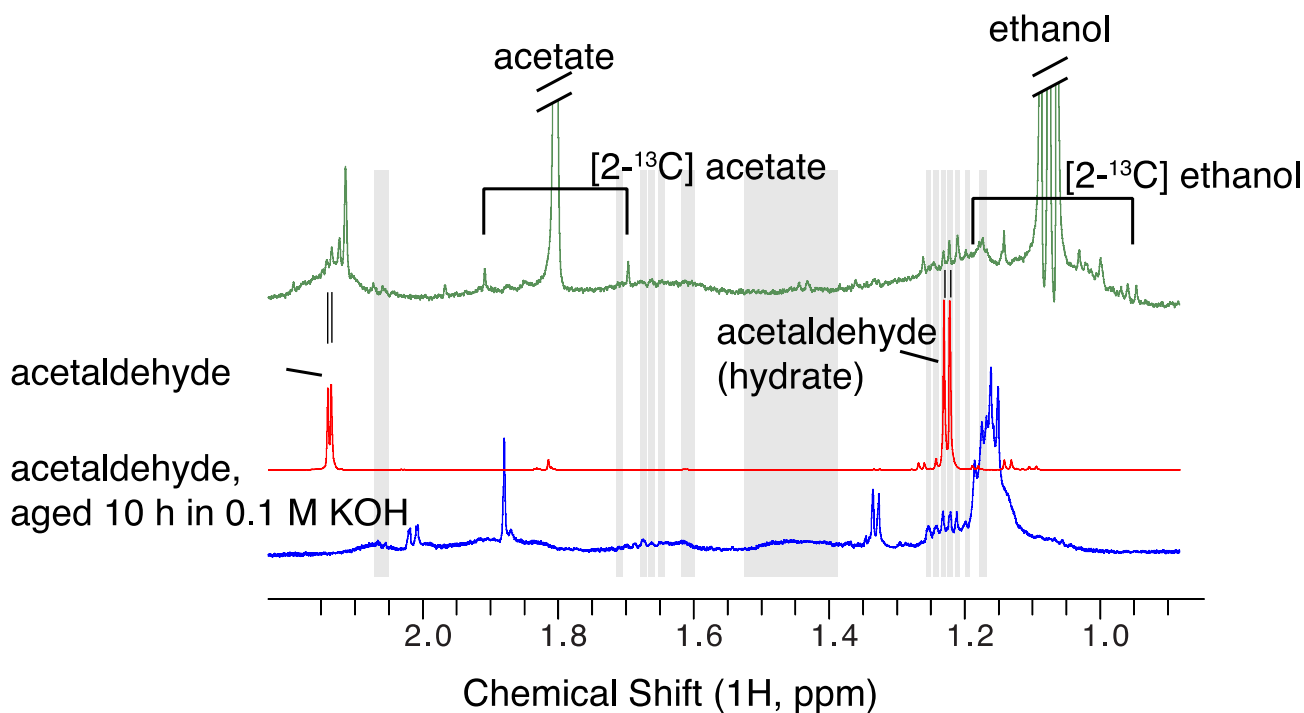


**Figure S.5.** Comparison of an electroreduction sample (green), and fresh (red) as well as aged (blue) 100 mM acetaldehyde solutions in 0.1 M KOH. Several signals and spectral features (humps) coincide between the aged acetaldehyde sample and the electroreduction sample, including minor signals from acetaldehyde. Methyl group satellites from natural abundance  $^{13}\text{C}$  acetate and ethanol are indicated as  $[2-^{13}\text{C}]$  acetate and  $[2-^{13}\text{C}]$  ethanol respectively.

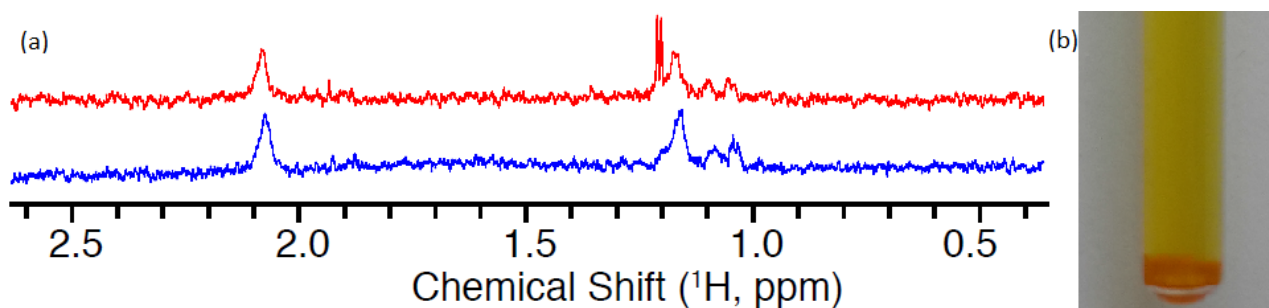


**Figure S.6.** (a) NMR spectra of 500  $\mu\text{M}$   $\text{CH}_3\text{CHO}$  prepared from 40 % (red) and 100 % (blue) acetaldehyde precursors. For acidified samples, two broadened signals can be observed, with chemical shifts 1.0-1.2 ppm and 2.05-2.1, respectively, for both samples. In the red spectrum, obtained from a standard made from 40 % acetaldehyde, aqueous acetaldehyde can also be identified as a sharp doublet at 1.2 ppm. This is not visible for the sample made from a 100 % precursor, as discussed further in section S.3 (b) Photo of NMR tube with 0.1 M acetaldehyde in 0.1 M KOH. The solution turns yellow, and a precipitate is formed at high concentrations.

## **S.4 Product Detection and Quantification**

Detection and quantification of gaseous products were carried out through automatic injection into a GC. Liquid products were analyzed using nuclear magnetic resonance (NMR) spectroscopy and static headspace-gas chromatography (HS-GC), the latter coupled with either a flame ionization detector (FID) or a mass spectrometer (MS).

### **GC and HS-GC-FID**

An Agilent 7890A was used when carrying out GC and HS-GC-FID. The injected gas was split 0.5:1 between a HP-PLOT Q column (Length: 45 m; ID: 0.53 mm; Film: 40.0  $\mu\text{m}$ ) eluting in a flame ionization detector (FID) and a HP-PLOT Molesieve column (Length: 30 m; ID: 0.53 mm; Film: 50.0  $\mu\text{m}$ ) eluting in a temperature conductivity detector (TCD).

Gaseous measurements were carried out at a constant temperature of 80 °C, utilizing both detectors.

For HS-GC-FID, an Agilent 7694E headspace sampler was used. Two glass vials were filled with 5 mL electrolyte each and sealed. In the headspace sampler, the liquid was heated to 70 °C during 15 minutes and the headspace gas composition subsequently injected automatically into the GC. Separation was carried out at 130 °C utilizing the FID only.

### **HS-GC-MS**

Volatile compounds were detected and analyzed by using an Agilent 7890B/5977 GC/MS. 5 ml of sample was added in 20 ml vial and stirred for 5 min at 70°C. A 2.5 mL PTFE Tipped Plunger Headspace Syringes (SGE Analytical Science) was used to extract 250  $\mu\text{l}$  of the vapor phase. A Solgel-wax column (Length: 30 m; ID: 0.25 mm; Film: 0.25  $\mu\text{m}$ ) was used for all analyses. The Split/Splitless injector was kept at 220°C, and set with a split ratio of 5:1.

The GC was kept at 40 °C for 4 min, and then increased to 250 °C with a rate of 6 °C/min. Helium was used as the carrier gas with a flow rate of 1.2 ml/min. The Agilent 5977 MS detector was operated in full scan mode at 70 eV with a scan range from 35 to 350 m/z.

Data analysis was performed using the software MassHunter WorkStation Software (Version B.07.00). Identification of compounds was based on comparison with a mass spectral database (NIST version 2.2) and confirmed with the relative pure standard. Each sample was analyzed in triplicate.

### **NMR spectroscopy**

NMR data was acquired at a Bruker Ascend 400 MHz spectrometer with Prodigy CryoProbe. A standard pre-saturated 1D NOESY experiment (noesypr1d) was used to acquire the 1D  $^1\text{H}$  spectra, in order to get adequate water suppression. Standard acquisition parameters were as follows; number of scans = 64, relaxation delay = 2 s,  $t_m$  = 20 ms, pre-saturation power level = 43 dB, spectral width = 20 ppm, and number of time domain points = 65k. 17 %  $\text{D}_2\text{O}$  and 0.5 mM of DMSO was added, the latter as an internal standard.

## S.5 Calibration

### GC

In order to obtain quantitative information from the product analysis techniques, a series of calibration measurements were carried out. For GC, a series of measurements on two standard gas mixtures were done, with the results shown in table S1. The compositions of the two were 5 % H<sub>2</sub> in Ar (AGA) and 0.2 % CH<sub>4</sub>, 0.15 % C<sub>2</sub>H<sub>6</sub>, 0.25 % C<sub>2</sub>H<sub>4</sub>, 0.15 % C<sub>3</sub>H<sub>8</sub>, 0.10 % C<sub>3</sub>H<sub>6</sub> and 1.00 % CO in Ar (AGA).

**Table 1:** GC calibration through injections of standard gas mixtures.

Gas	% in Sample gas	Injection 1	Injection 2	Injection 3	Average	Signal for 1%
CH <sub>4</sub>	0.2	5069	5052		5061	25304
C <sub>2</sub> H <sub>4</sub>	0.25	12930	12860		12895	51580
C <sub>2</sub> H <sub>6</sub>	0.15	7528	7476		7502	50014
H <sub>2</sub>	5	5665	5650	5557	5624	1125

### HS-GC

Ethanol and acetaldehyde were the only two volatile liquid products present in our samples, detectable by HS-GC. 1 mM, 500 μM, 250 μM and 50 μM solutions of ethanol and acetaldehyde in 0.1 M KOH matrix, as well as a blank solution of 0.1 M KOH were prepared. Three samples at each concentration were injected with HS-GC-FID, with the resulting data shown in figure S.4.

It is worth noticing that there is a certain spread between the measurement points at each concentration. The long tail of the ethanol peak (see figure S.9) gives an uncertainty in the integration, particularly for low concentrations. Minor leaks from the HS-GC vials can also explain this error. The sharp acetaldehyde peak gives accurate integration. However, there will be some error due to evaporation because of its high volatility. This is particularly relevant for concentrated solutions, such as the 40 % acetaldehyde in water (Sigma Aldrich) used here. Even though it was stored in a refrigerator, we observed the acetaldehyde content to drop over time. Hence, it is important to use a fresh solution. As discussed in the main text, uncertainty in the calibration for liquid product analysis could help explain the deviations from 100 % observed for the total Faradaic efficiency in some cases.

### NMR spectroscopy

Acetaldehyde was not visible in routine NMR measurements on CO reduction samples. Hence, ethanol and acetate were the only compounds that needed calibration. Samples with 1000, 500, 250 and 50 μM ethanol and acetate in 0.1 M KOH were measured, yielding the calibration curves shown in figure S.5. Acetate, which is the only product that was quantified through NMR spectroscopy, exhibits an intense singlet peak, and is non-volatile, giving minimal error in the calibration.

It is worth noticing that two different types of standard solutions of acetaldehyde, ethanol and acetate were prepared. One was made from a 40 % solution of acetaldehyde in H<sub>2</sub>O (Sigma Aldrich). The other one was made from 100 % acetaldehyde (≥ 99.5 %, Fluka, anhydrous) that was diluted to 20 % in H<sub>2</sub>O for easier handling. As shown in figure 2 (c) in the main article and figure S.3, acetaldehyde can only be detected in the solution made from 40 % with NMR spectroscopy. The chemistry of acetaldehyde and its appearance in NMR spectra is discussed further in section S.2.

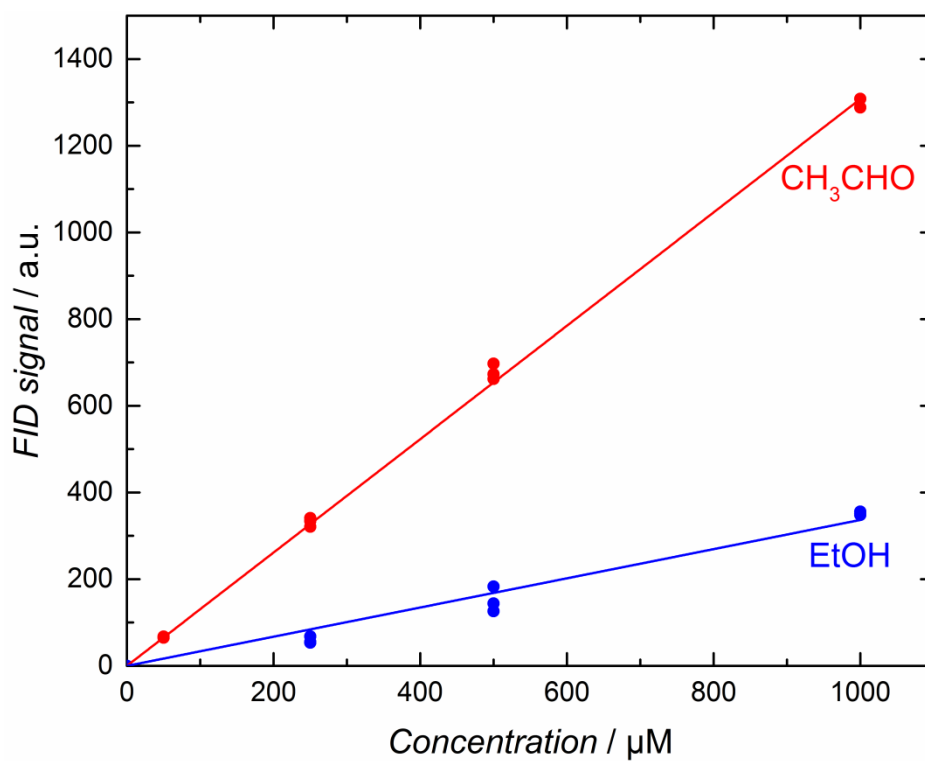


**Figure S.7.** HS-GC-FID calibration curves. Standards of 1000, 500, 250 and 50  $\mu\text{M}$  acetaldehyde, ethanol and acetate were measured in triplicates. Acetate is non-volatile, thus not detectable with HS-GC. Calibration curves are shown for ethanol (blue) and acetaldehyde (red). The larger uncertainty in the ethanol calibration can be partly attributed to the long tail of its peak, inducing errors in the integration.

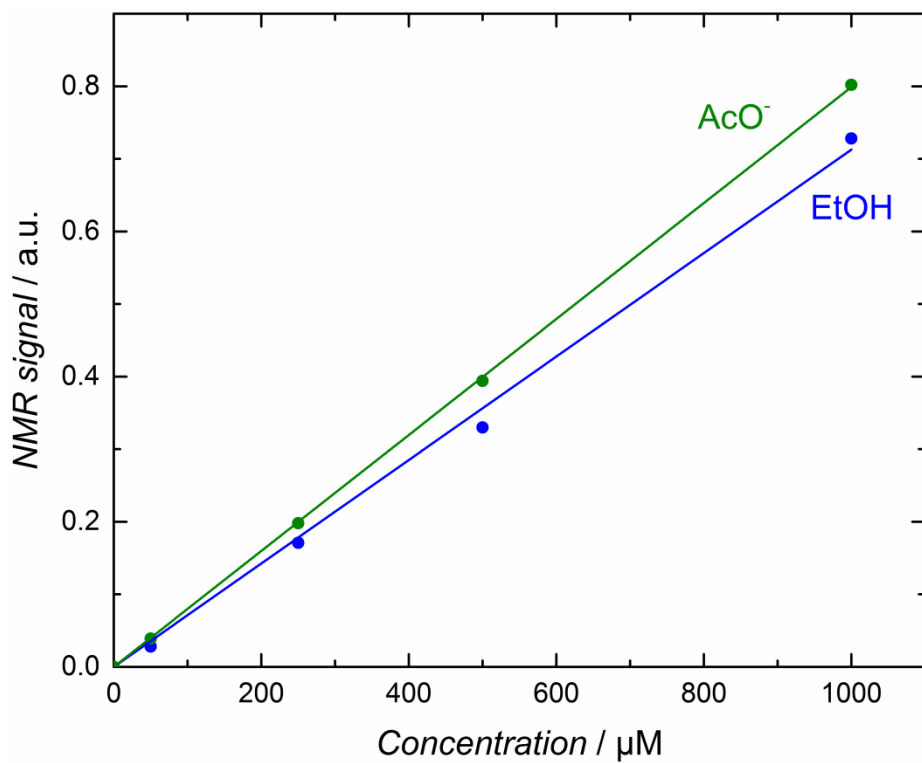


**Figure S.8.** NMR spectroscopy calibration curves. Standards of 1000, 500, 250 and 50  $\mu\text{M}$  acetaldehyde, ethanol and acetate were measured. Acetaldehyde cannot be identified in NMR spectra from CO reduction samples, as described throughout this work, and is not included. Calibration curves are shown for ethanol (blue) and acetate (green).

## S.6 Electrochemical Measurements

All electrochemical measurements were carried out in a custom-built three electrode glass cell. A gold mesh was used as counter electrode (CE), with the working electrode (WE) and CE compartments separated by a Nafion® 117 proton conducting membrane. Electrochemical measurements were carried out using a BioLogic VMP2 potentiostat, controlled through the EC-Lab software.

A Hg/Hg<sub>2</sub>SO<sub>4</sub> reference electrode (RE) was used, separated from the WE compartment with an ion-conducting ceramic frit. The RE was referred to the reversible hydrogen electrode (RHE) using the following equation (S.3). All potentials given throughout the work are converted to this scale.

$$E \text{ (vs. RHE)} = E \text{ (vs. Hg/Hg}_2\text{SO}_4) + 0.633 \text{ V} + 0.059 \text{ V} * \text{pH} \quad (\text{S.4})$$

The second term on the right side of the equation, 0.633 V, is the offset of the Hg/ Hg<sub>2</sub>SO<sub>4</sub> RE at 0 V vs. RHE. It was measured through the onset of the hydrogen evolution reaction (HER)/hydrogen oxidation reaction (HOR) on a Pt electrode in 0.1 M KOH.

Before all measurements, the ohmic drop was measured using electrochemical impedance spectroscopy, reaching typical values of 20-50 Ω, depending on the position of the WE relative to the RE, among other factors. 85 % of the ohmic drop was compensated for in the software. For measurements at -0.28 V and -0.33 V, the last 15 % were insignificant (≤ 10 mV). However, for measurements set to -0.43 V, the last 15 % of the ohmic drop typically corresponds to 35-45 mV and corrections were carried out post-experiment.

CO reduction experiments were carried out potentiostatically in 0.1 M KOH (Fluka TraceSELECT®, ≥ 99.995 %) saturated with 1.1 bar CO (AGA). Acetaldehyde hydrogenation experiments were carried out with 10 mM acetaldehyde (≥ 99.5 %, Fluka, anhydrous) added to the 0.1 M KOH electrolyte saturated with 1.1 bar Ar (AGA)

The WE compartment of the measurement cell is connected through a glass bubbler to a gas loop, directly connected to the sample loop of the gas chromatographer (GC). During measurements, this loop is closed, enabling accumulation of any gaseous products in order to increase sensitivity. A pump is installed, circulating the headspace gas through the loop and the electrolyte during measurements.

## S.7 Computational Details

DFT calculations were performed on a 4x3x3-atom periodic computational cell corresponding to the (211) facet of fcc Cu, with a 4-atom long step edge. This system was chosen due to the presence of step edge, four-fold, and three-fold terrace sites that may occur on OD-Cu. Electronic energies were determined with the Dacapo DFT calculator as implemented in the open-source Atomic Simulation Environment (ASE),<sup>[8]</sup> and the revised Perdew-Burke-Ernzerhof (RPBE) exchange correlation functional was chosen for its relative accuracy in describing chemisorption energies.<sup>[9]</sup> In addition, we used parameters of 340 and 500 eV for the plane wave and density cutoff energies with a Fermi-level smearing width of 0.1 eV and a (4,4,1) Monkhorst-Pack k-point sampling mesh.<sup>[10]</sup>

As stated in the main text, geometries of multiple configurations of each adsorbate corresponding to placement on each available binding site were optimized into local energy minima such all forces were below 0.05 eV/Å. The most stable configuration for each adsorbate was selected for the energies presented in the free energy diagram, and a free energy correction corresponding to vibrational contributions determined in the harmonic approximation was also applied to each adsorbate. Free energies of gas-phase species at standard conditions were determined using the ideal-gas approximation, and the free energy of liquid water was determined using the gas-phase energy of H<sub>2</sub>O at the appropriate vapor pressure.<sup>[11]</sup> The free energy of solvated acetaldehyde was calculated using a Henry's law constant of  $7.89 \times 10^{-5} \text{ atm m}^3 \text{ mol}^{-1}$ .<sup>[12]</sup>

Solvation corrections to individual adsorbates are also included based on the chemical identity of each adsorbate, similar to previous work from Peterson et al.<sup>[13]</sup> in which R-O groups were assigned a 0.1 eV stabilization and R-OH groups assigned a 0.25 eV stabilization. We apply these corrections to each adsorbate, with a 0.1 eV stabilization for each aldehyde group present on a given adsorbate and a 0.25 for each hydroxyl group. For example, OCHCHO would have two stabilization energies from the aldehyde groups, totalling a 0.2 eV stabilization, while CH<sub>3</sub>CHOH is assigned a 0.25 eV stabilization for the one hydroxyl group.

## S.8 Full HS-GC-FID chromatogram and NMR spectrum

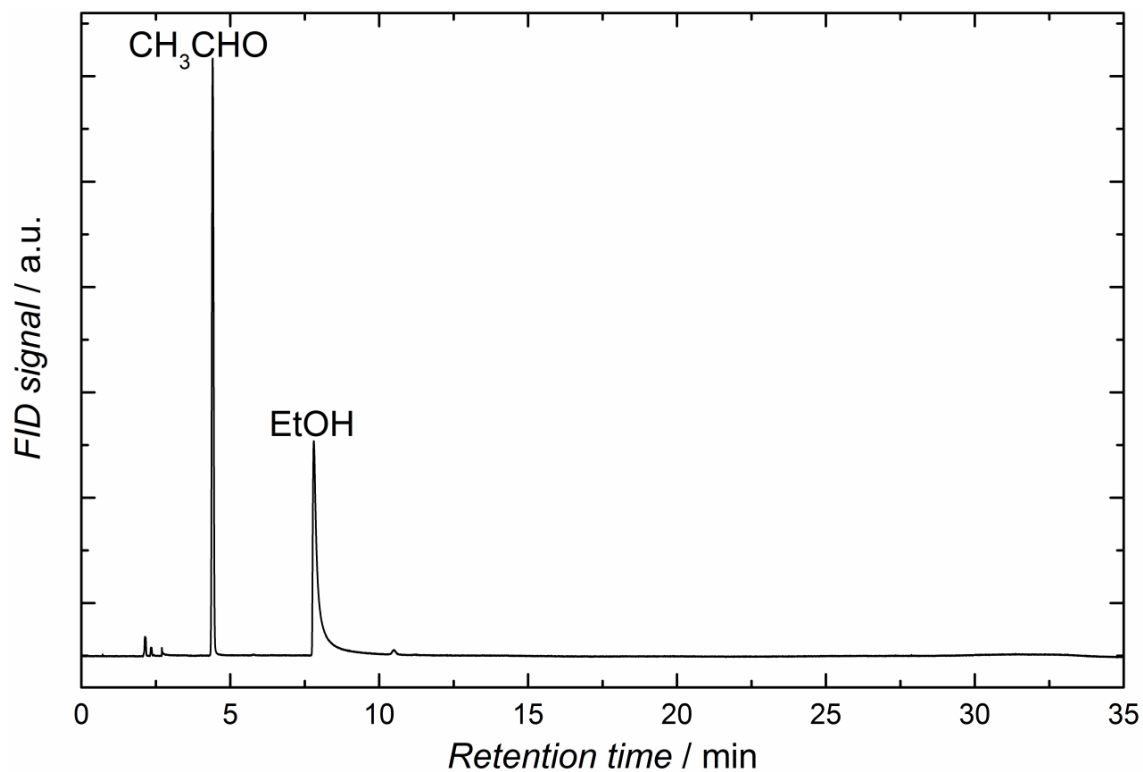


**Figure S.9.** Full HS-GC-FID spectrum from a representative CO reduction sample measured at -0.33 V. Acetaldehyde and ethanol are the only major products. The minor peaks around 2.5 min are caused by dissolved hydrocarbon gases such as methane and ethylene. They are present in trace amounts in both the CO gas and the atmosphere.



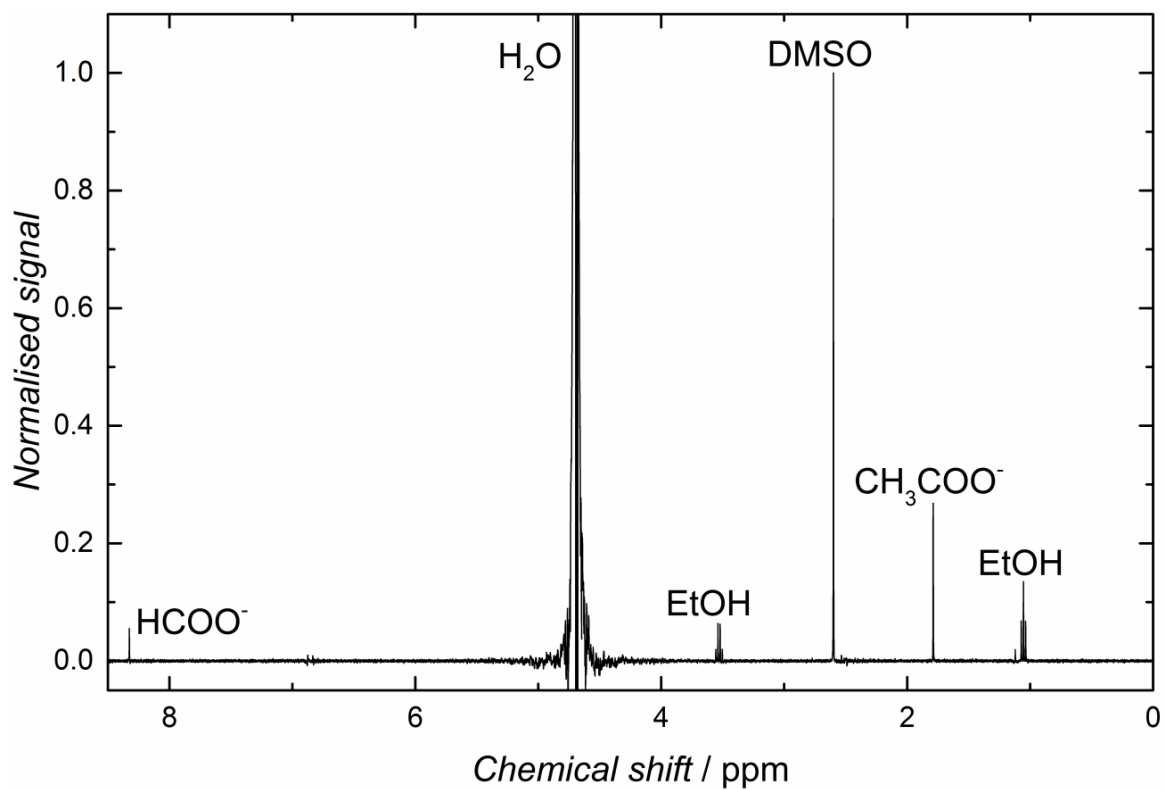


**Figure S.10.** Full NMR spectrum for a representative CO reduction sample at -0.33 V. A triplet and a quartet at 1.1 and 3.6 ppm are attributed to ethanol. Acetate can be seen through a singlet at 1.8 ppm, while the intense singlet at 2.7 ppm is caused by DMSO, used as an internal standard. Formate is also present in trace amounts, identified through a singlet at 8.4 ppm.

## Bibliography

- [1] C. W. Li, J. Ciston, M. W. Kanan, *Nature* **2014**, *508*, 504–507.
- [2] K. J. P. Schouten, E. P. Gallent, M. T. M. Koper, *J. Electroanal. Chem.* **2013**, *699*, 6–9.
- [3] Y. Kwon, S. C. S. Lai, P. Rodriguez, M. T. M. Koper, *J. Am. Chem. Soc.* **2011**, *133*, 6914–6917.
- [4] T. A. Geissman, in *Org. React.*, Wiley-VCH, **2011**, pp. 94–113.
- [5] J. McMurry, *Organic Chemistry*, Brooks/Cole, **2004**.
- [6] R. D. Harrison, *Revised Nuffield Advanced Science Book of Data*, Longman, **1984**.
- [7] E. F. Degering, T. Stoudt, *J. Polym. Sci.* **1951**, *7*, 653–656.
- [8] S. R. Bahn, K. W. Jacobsen, *Comput. Sci. Eng.* **2002**, *4*, 56–66.
- [9] B. Hammer, L. Hansen, J. Nørskov, *Phys. Rev. B* **1999**, *59*, 7413–7421.
- [10] H. J. Monkhorst, J. D. Pack, *Phys. Rev. B* **1976**, *13*, 5188–5192.
- [11] C. J. Cramer, *Essentials of Computational Chemistry: Theories and Models*, Wiley-VCH, **2013**.
- [12] U.S. Environmental Protection Agency, “Chemical Summary of Acetaldehyde,” can be found under [http://www.epa.gov/chemfact/s\\_acetal.txt](http://www.epa.gov/chemfact/s_acetal.txt), **1994**.
- [13] A. A. Peterson, J. K. Nørskov, *J. Phys. Chem. Lett.* **2012**, *3*, 251–258.